MicroRNA microarray
Methods are as described in text. For full description, see Chen et al.[1]

RNA extraction
Methods are as described in text.

Real-time RT-PCR quantification of microRNA expression
To detect and quantify mature microRNA expression in erythrocytes, we used TaqMan miRNA assays (Applied Biosystems) according to manufacturer's directions and as previously described.[2] Briefly, 500ng total RNA was used in each reaction and mixed with the RT primer (total 15 uL). The reverse transcription reaction was carried out and 1.33 uL of cDNA was used for PCR reaction along with TaqMan primers (20uL total). Real-time PCR reactions, including no-template controls, were conducted in triplicate using the ABI 7500 real-time PCR system. Results were analyzed and expressed as C_T (threshold cycle) values, and relative expression was calculated using the comparative C_T method.[3] Unless otherwise specified, we compared relative levels of microRNA with probes specific for the indicated mature microRNA using total RNA and normalized by cell number.

For the second independent cohort of patients (Fig. 6, Table S2) we used 250 ng total RNA and determined the absolute miR-144 expression per cell by real-time PCR as described above with synthesized miR-144 (Dharmacon) as standards.

To detect and quantify mature microRNA expression in K562 cells expressing expression constructs, we used TaqMan miRNA assays (Applied Biosystems) according to manufacturer's directions. Briefly, 1ug total RNA was used in each reaction and mixed with the RT primer (total 15 uL). The reverse transcription reaction was carried out and 1.33 uL of cDNA was used for the PCR reaction along with TaqMan primers (20uL total). Real-time PCR reactions, including no-template controls, were conducted in triplicate using the ABI 7500 real-time PCR system. Results were expressed as CT (threshold cycle) values, analyzed using the standard curve method, and normalized by RNU6 expression.

Real Time RT-PCR quantification of mRNA expression
RNA was reverse-transcribed with SuperScript II following manufacturer's protocol (Invitrogen). cDNAs were then used as the substrate for gene expression level measurements by qPCR with Power SYBRGreen PCR mix (Applied Biosystems) and primers specific for SOD1, CAT, GCLC, and GCLM, with GAPDH as an internal control.

Cell culture, cell transfection
HEK-293 cells (ATCC) were maintained in DMEM with 10% fetal bovine serum, glutamine, and antibiotics. K562 cells (ATCC) were maintained in standard RPMI 1640 supplemented with 10% fetal bovine serum, glutamine, and antibiotics. Transfection experiments with K562 cells were done using Amaxa nucleofection (Amaxa) or Lipofectamine LTX (Invitrogen) according to the respective protocols suggested by manufacturers. Primary erythroid cell transfection was done using Amaxa nucleofection.

Luciferase assay
HEK-293T cells were cotransfected with 0.2 μg of indicated reporter, 20 ng Renilla luciferase construct and 2 μg of indicated microRNA expression constructs using Lipofectamine 2000 (Invitrogen). All samples were assayed in triplicate. After 24 hours, the transfected cells were washed and lysed with passive lysis buffer (Promega). Firefly and Renilla luciferase activity were measured using the Dual-Glo Luciferase assay (Promega) and a luminometer (Lumat, Berthold Technology).

Glutathione assay
Intracellular glutathione concentration was measured using the GSH-GLO Glutathione assay (Promega) according to manufacturer's instructions, based on the conversion of a luciferin derivative into luciferin in the presence of glutathione and catalyzed by glutathione S-transferase. For the erythrocyte lysate experiments, the amount of glutathione was expressed as micromolar concentration per cell. All samples were assayed in triplicate.

Superoxide dismutase assay
Total superoxide dismutase (SOD) was assessed using an assay that measures the dismutation of superoxide radicals generated by xanthine oxidase and hypoxanthine (Cayman Chemical). One unit of SOD was defined as the amount of enzyme needed to exhibit 50% dismutation of the superoxide radical. All samples were assayed in triplicate and immediately analyzed for absorbance at 450nm by microplate reader (FLUOstar OPTIMA, BMG LabTech).

Western blot analysis
Cells were lysed and supplemented with protease inhibitor cocktail (Roche Applied Science) followed by sonication and cold centrifugation. Equal volumes of sample buffer were added to 12 or 25 ug of sample, boiled, resolved on a 7.5% or 10% Tris-HCl gel (Bio-Rad), and transferred onto polyvinylidene fluoride (PVDF) membrane (Hybond-P, GE Healthcare). NRF2 protein was detected using anti-NRF2 monoclonal antibody (Santa Cruz Biotechnology) followed by horseradish peroxidase (HRP)-conjugated goat anti-rabbit IgG antibody (Abcam). The western blot was then visualized by enhanced chemoluminoscence (Western Lightning-ECL Plus, PerkinElmer) and exposure to film. Images were digitized by scanner. To control for protein loading, the membranes were stripped (Restore Plus, Thermo Scientific) and reprobed with goat anti-rabbit antibody to beta-tubulin (Abcam) or GAPDH (Santa Cruz). Densitometric measurements were performed with ImageJ software (http://rsb.info.nih.gov/ij/).

Reactive oxygen species assay
For ROS measurement, erythrocytes were washed twice with PBS, resuspended to 2% packed cell volume, and incubated in 500uM H_2O_2 in a CO_2 incubator (37C, 5% CO2) for 1 hour. Cells were then resuspended in PBS and HEPES buffer and incubated with 5-(and-6)-chloromethyl-2′,7′-dichlorodihydrofluorescein diacetate, acetyl ester (CM-H_2DCFDA) probe (Molecular Probes) for 30 minutes. Samples were immediately assayed by flow cytometry (FACScan, BD Biosciences) and analyzed by the CellQuest program (BD Biosciences). Results are reported as differences in mean fluorescence intensity. All samples were assayed in triplicate.

Expression constructs
The NRF2 3′UTR-luciferase reporter, NQO1-ARE-luciferase reporter, NRF2 cDNA expression, and miRNA expression constructs referred to in the supplemental methods are as described in text.

The NRF2 3′UTR mutant reporters were constructed with QuikChange II Site-Directed Mutagenesis (Stratagene, CA), which created base pair changes in the miR-144 seed sequence-targeted regions **(**site 1: tttata**ctg**ttcttat to tttata**gaa**ttcttat and site 2: aaata**c**tgtatgga to aa**c**tact**g**tg**t**atgga**).**

Overexpression construct amplification primers: miR-144 (forward: gaagctgtgtgtgtccagcc; reverse: gcagcatctctcctgtcctc), miR-142-5p (forward: gcggccagccaggggttc; reverse: tccacgtaccatcccttcc), miR-320 (forward: caggaaccagacagggacgc; reverse: ccgactcttaagtccaggtc**).**

The si-NRF2 for knockdown of NRF2 was purchased from Dharmacon, along with 'si-control' for transfection control.

Additionally, miR-144-seedmut1 was made by taking the miR-144 pcDNA-based expression construct and performing site-directed mutagenesis with QuikChange II Site-Directed Mutagenesis (Strategene) using primers **(forward:** 5′-tgtaagtttgcgatgagacactattctatagatgatgtactagtccggg-3′**; reverse:** 5′-cccggactagtacatcatctatagaatagtgtctcatcgcaaacttaca-3′ **)** to encode the following changes (underlined) in the seed region (in bold) of miR-144: U**ACAGUAU**AGAUGAUGUACU => U***A<u>UUC</u>*****UAU**AGAUGAUGUACU . This construct is endogenously processed to produce mature miR-144 with a mutated seed region and thus serves as a control for specificity of the miR-144 sensor for measuring the mature form of miR-144.

The NRF2-without-3UTR expression construct was made by digesting out the 3UTR and 72bp of the ORF from the NRF2 cDNA expression plasmid (Origene) using PstI and XbaI. The 72bp ORF was added back by annealing, digesting, and ligating the following oligo and its complement into the PstI/XbaI site

Mature miR-144 expression assay using sensor construct for mature miR-144
Two reverse complement 'target' sites for mature miR-144 were cloned in tandem between the XhoI and NotI sites of the si-CHECK-2 luciferase reporter plasmid (Promega), which encodes both the firefly luciferase gene as the internal control for transfection and renilla luciferase gene as the reporter. The sensor assay is performed by cotransfection of the sensor construct with indicated expression constructs into K562 cells using Lipofectamine LTX (Invitrogen) followed by Dual Luciferase assay (Promega) performed according to manufacturer's instructions. Each sensor assay is performed alongside a control assay cotransfecting the 'empty' no-insert siCHECK-2 luciferase reporter plasmid under the same conditions. The relative difference between the no-insert reporter and the sensor construct is reported.

REFERENCES

1. Chen SY, Wang Y, Telen MJ, Chi JT. The genomic analysis of erythrocyte microRNA expression in sickle cell diseases. *PLoS ONE* [Electronic Resource]. 2008;3:e2360.
2. Chen C, Ridzon DA, Broomer AJ, et al. Real-time quantification of microRNAs by stem-loop RT-PCR. *Nucleic Acids Research*. 2005;33:e179.
3. Schmittgen TD, Livak KJ. Analyzing real-time PCR data by the comparative CT method. *Nat Protocols*. 2008;3:1101–1108.

Figure S1. Detailed heatmap for the expression of reticulocyte microRNA in the two groups of HbSS patients

The expression value of the reticulocyte specific microRNAs determined using TLDA in a previous study was extracted and arranged in hierachical clustering and shown for two groups of HbSS.

Figure S2. MicroRNA expression in HbAA compared to HbSS erythrocytes

(A) MiR-144 and miR-142-5p were overexpressed in HbSS erythrocytes compared to normal (HbAA) erythrocytes, as shown by microRNA microarray expression analysis. MiR-451 was also expressed at a significantly higher level in group I HbSS patients. However, a subset of HbSS patients HbSS-I (n=4) had greater miR-144 and miR-142-5p expression compared to subset HbSS-II (n=8) (A), but less consistently so for miR-451. (B) MiR-144 overexpression in HbSS (n=18) vs HbAA (n=3) was confirmed by quantitative real-time PCR analysis using the patient sample set as described in Fig. 5 and TableS2. (C) The heterogeneity among HbSS patients was also confirmed by quantitative Real-time PCR analysis: HbAA (n=3) vs. HbSS 'low miR-144 (n=9) vs. HbSS 'high miR-144 (n=9). The HbSS 'low miR-144' group was not significantly different from HbAA (p=.95) in miR-144 expression, while the HbSS 'high miR-144' group showed significantly higher (p=.002) miR-144 expression compared to HbAA. Data is shown here alongside HbAA miR-144 expression data. Individual miR-144 expression data for each HbSS sample in this dataset is shown in Fig. 5C and Table S2.

Figure S3. Validation of microRNA overexpression constructs using quantitative Real-Time PCR

(A) K562 cells were transiently transfected with expression constructs for miR-144 and miR-142-5p (line constructs). After RNA extraction, mature microRNA levels were measured using real-time PCR. (B) Relative to empty vector, cells transfected with the miR-144 construct overexpressed miR-144 by 5.7 fold (± 1.60 SEM p=.0011). MiR-451, due to its close proximity to miR-144 precursor (92bp apart), was also measured as a control, and its expression was not significantly different (from that of empty vector) in the cells expressing the miR-144 construct (.891 fold ±.124 SEM, p=.0010). Thus we were able to significantly overexpress mature miR-144. (C) MiR-144 expression was further validated using a miR-144 sensor construct. The sensor was transfected alone (mock) or cotransfected with pcDNA (empty vector), miR-144, miR-320, or miR-144-seedmut1 expression vectors into K562 cells by Lipofectamine LTX lipofection method as described in text. Cotransfection with miR-144 expression vector showed significant repression (83.5% ± .80 SEM p<.0001) of miR-144 sensor luciferase reporter activity (relative to empty vector). Expression of empty vector, miR-144-seedmut1, and miR-320 did not significantly repress luciferase activity of the miR-144 sensor construct compared to mock transfection. (D) Relative to empty vector, cells with the miR-142-5p construct overexpressed miR-142-5p by 1.96 fold (± .097 SEM, p=.0011). Validation of the miR-320 expression construct is described in Chen et al.[1]

Figure S4. miR-144 represses the NRF2-3UTR reporter in HEK293 cells

When expression constructs for miR-144, miR-142-5p and miR-320 (Fig. S2) were co-transfected with the NRF2 3′UTR reporter construct (upper panel) into HEK293 cells to measure the effect of their respective overexpression on luciferase reporter activity, we found (lower panel) that both miR-144 and miR-142-5p were able to significantly repress luciferase activity

by 64.2% (± 9.9 SEM p=.0029) and 37.0% (± 13.7 SEM p=.036) respectively. MiR-320, which does not have a target site in the NRF2 3′UTR, did not have significant effect on luciferase activity. Thus, NRF2 is a direct regulatory target of miR-144 through the specific interaction between miR-144 and its predicted target sites within the NRF2 3′UTR.

Figure S5. MiRNA effect on NRF2 protein expression in erythroid cells
(A) Baseline NRF2 expression in K562 cells with miR-144 or miR-320 overexpression in comparison to that of empty vector control and relative to beta-tubulin loading control. (B) The NRF2 expression after 6 hours of 10uM H202-induced oxidative stress in K562 cells with miR-144 or miR-320 overexpression was determined by Western blots in comparison to that of empty vector control and relative to beta-tubulin loading control.

Figure S6. Primary erythroid cell transfection and NRF2 protein expression
Successful transfection of D8 primary erythroid cells with GFP vector compared to mock transfected cells by Amaxa.

Figure S7. ARE luciferase reporter assay
(A) The NQO1-ARE luciferase reporter construct was validated in K562 cells using NRF2 cDNA overexpression construct as a positive control, which led to a 40.85 fold increase in luciferase activity compared to mock-transfected cells. The downregulation endogenous NRF2 via gene silencing by siRNA against NRF2 leads to a 73.3% decrease in ARE-reporter activity compared to mock-transfected cells and 43.2% decrease compared to si-control transfected cells. (B) The NQO1-ARE luciferase reporter construct was cotransfected with empty vector, miR-144, or NRF2 (as a positive control) into HEK293 cells to measure their respective effects on ARE-driven gene expression. We found that miR-144 (relative to vector control) significantly inhibited activity of the ARE luciferase reporter by 56.8% (±4.4 SEM, p<.0001), while NRF2 overexpression significantly increased reporter activity.

Figure S8. MiRNA effect on baseline expression of ARE-driven genes and glutathione
(A) To further confirm the effect of miR-144 overexpression on the RNA expression of several ARE-driven genes under oxidative stress, we measured the gene expression of SOD1, CAT, and the catalytic (GCLC) and modulatory (GCLM) subunits of GCS at baseline (Fig S7A) and after treatment with H_2O_2-induced oxidative stress (Fig. 4B) in K562 erythroid cells. At baseline, miR-144 overexpression led to an 18.2% decrease in CAT expression (±2.3 SEM, p=.001), and 10.0% increase in GCLM expression (±3.0 SEM, p=.0021) in K562, and did not significantly affect the expression of SOD1 or GCLC. (B) Under basal conditions, NRF2 overexpression led to an increase in glutathione concentration ([GSH]) of 73.5% (Fig. 4C) while miR-144 overexpression did not lead to significant changes in [GSH].

Figure S9. Flow cytometry GCSM intracellular staining of HbSS RBCs
Representative original flow cytometry data from the intracellular staining of GCSM in mature erythrocytes of HbSS individuals with high or low miR-144 levels from Fig. 5E is shown here. Intracellular assay materials and methods are as noted in main text.

Figure S10. Oxidative stress indicators among HbSS (high miR-144 vs. low miR-144) and in HbSS vs. HbAA erythrocytes

(A) Although intracellular SOD1 protein expression was higher in the 'low miR-144' (n=3) compared to the 'high miR-144' (n=3) group, this difference did not reach statistical significance (p=.0956). Values expressed in mean fluorescence intensity (MFI) (B) HbSS erythrocytes had significantly decreased (34.3%, p<.0001) glutathione levels compared to normal HbAA erythrocytes. The graph in (B) is representative of three experiments using HbAA (n=3) and HbSS (n=4) erythrocyte lysate samples. (C) HbSS erythrocytes had significantly increased (-54.5%, p=.047) reactive oxygen species levels compared to HbAA erythrocytes, reported as mean fluorescence intensity (MFI) of the ROS-detecting probe CM-H_2DCFDA. The graph in (B) is representative of three experiments using HbAA (n=4) and HbSS (n=4) erythrocytes.

Figure S11. Erythroid maturation of HbSS and HbAA CD34 progenitors

(A) May-Grunwald-Giemsa staining of cells in culture at day 8, 10, 12, and 14 of erythroid maturation in HbAA and HbSS progenitors. (B) Fold change in miR-144 expression at the indicated day of differentiation relative to Day 8 levels in HbAA (n=3) and HbSS (n=2) progenitors. (C) NRF2 protein levels were lower in HbSS compared with HbAA erythroid cells during differentiation. Both HbAA and HbSS samples respectively demonstrated significant decrease in NRF2 expression between D8 and D10 (p=.021, p<.0001), D12 (p<.0001, p=.0002), and D14 (p=.026, p=.013). In HbAA samples, expression change between D10 and D12 is statistically significant (p=.049). Expression change between D12 and D14 is not significant (p=.06). In HbSS samples, expression changes between D10 and D12 (p=.45), D12 and D14 (p=.27) are not significant.

Figure S1

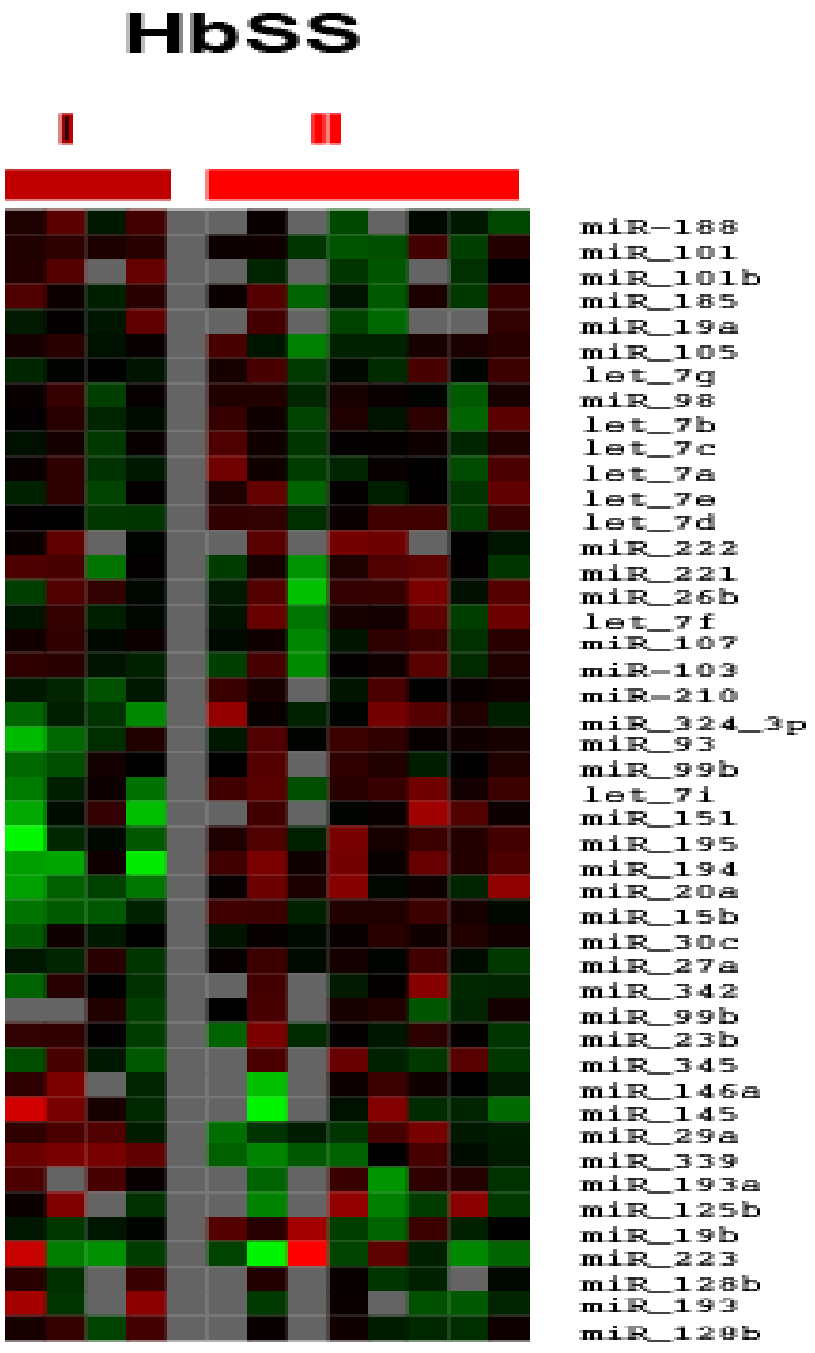
HbSS
I
II
miR-188
miR_101
miR_101b
miR_185
miR_19a
miR_105
let_7g
miR_98
let_7b
let_7c
let_7a
let_7e
let_7d
miR_222
miR_221
miR_26b
let_7f
miR_107
miR-103
miR-210
miR_324_3p
miR_93
miR_99b
let_7i
miR_151
miR_195
miR_194
miR_20a
miR_15b
miR_30c
miR_27a
miR_342
miR_99b
miR_23b
miR_345
miR_146a
miR_145
miR_29a
miR_339
miR_193a
miR_125b
miR_19b
miR_223
miR_128b
miR_193
miR_129b

Figure S2

A.

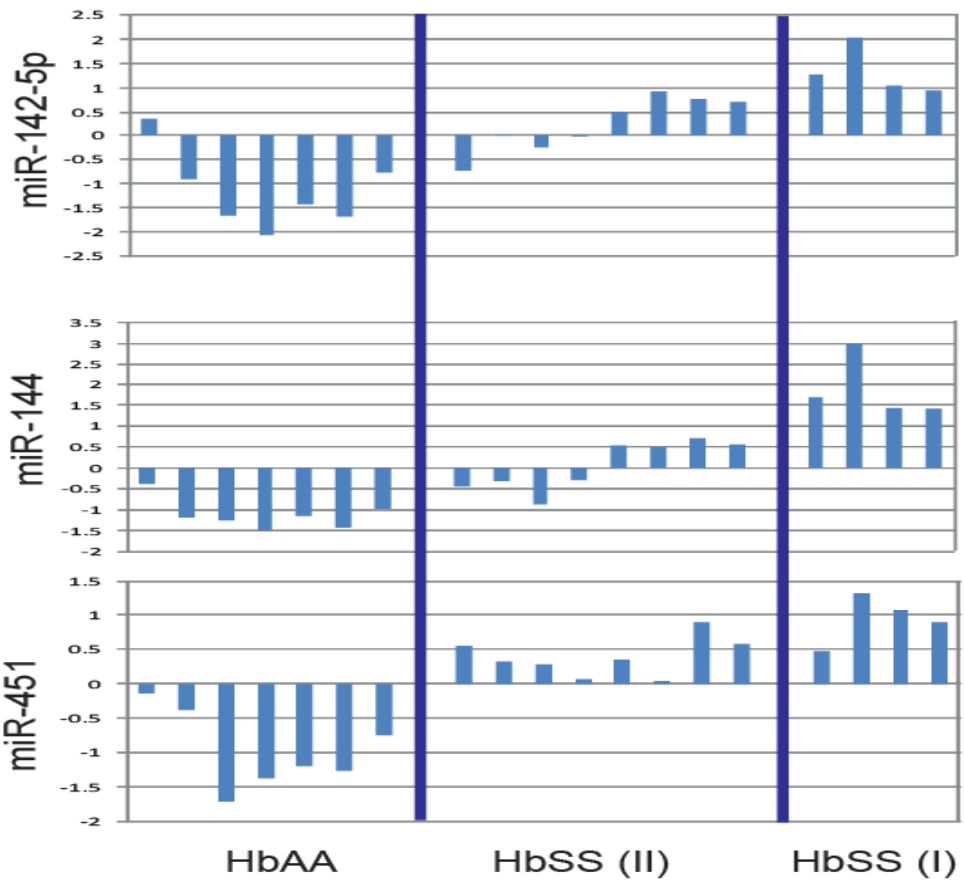

B.

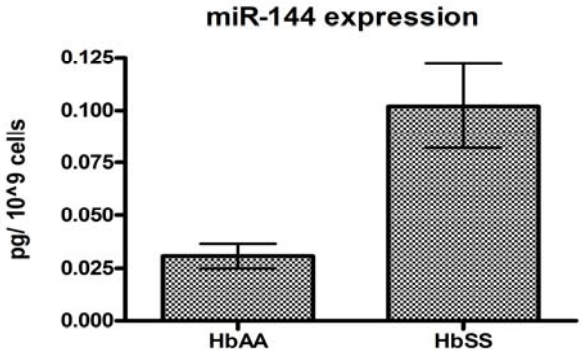

C.

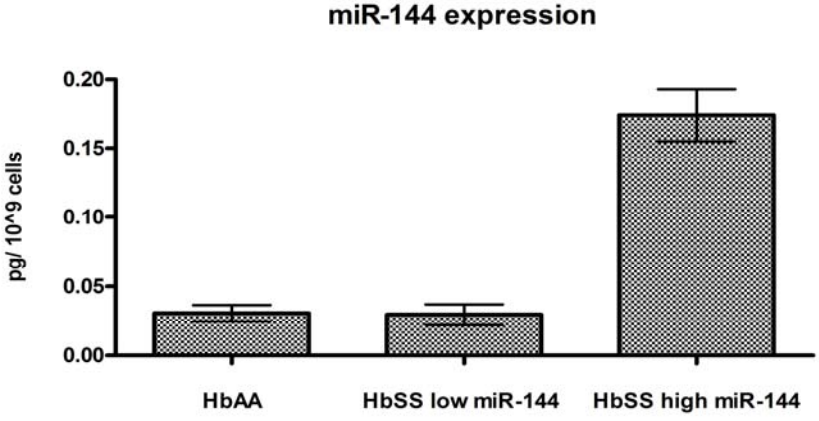

Figure S3

A.

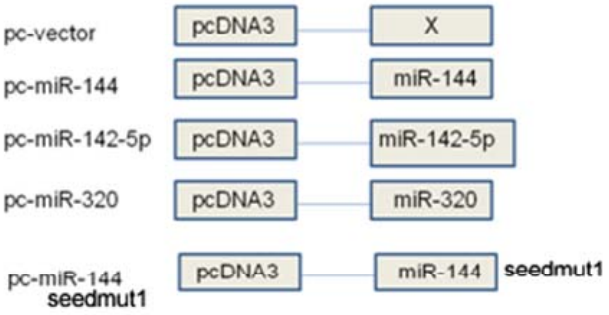

B.

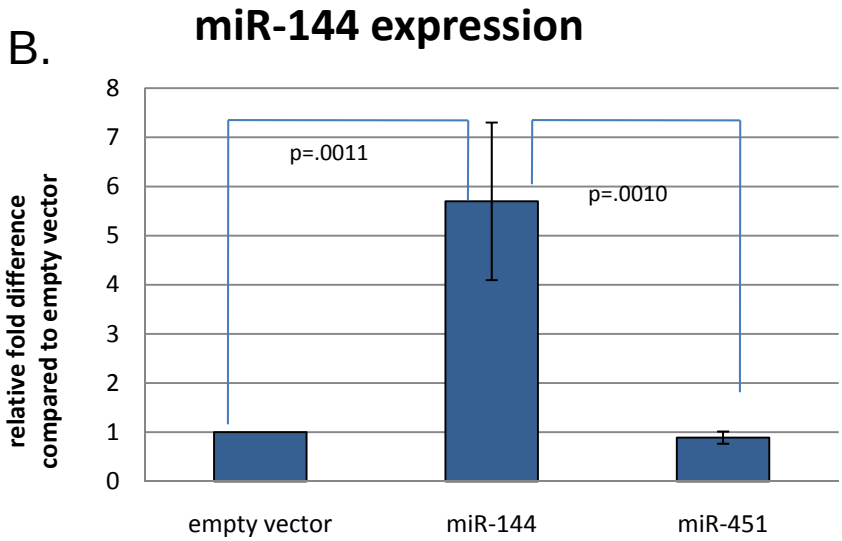

C.

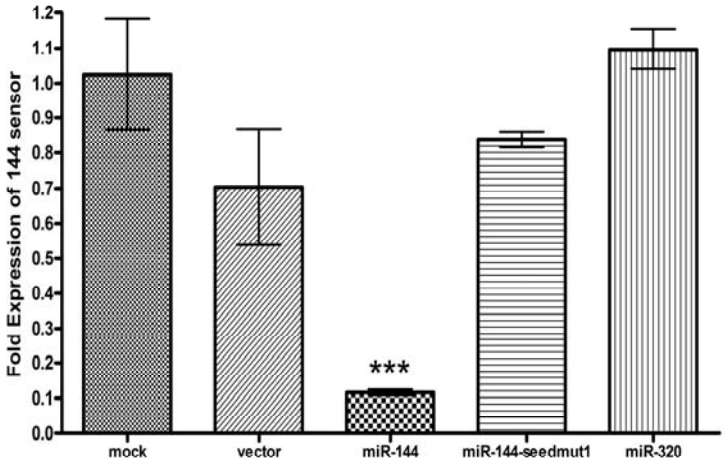

D.

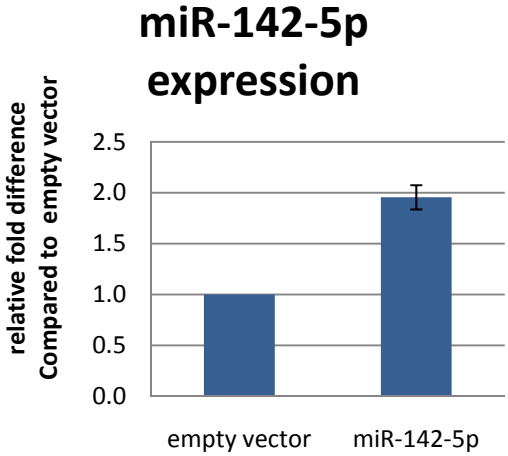

Figure S4

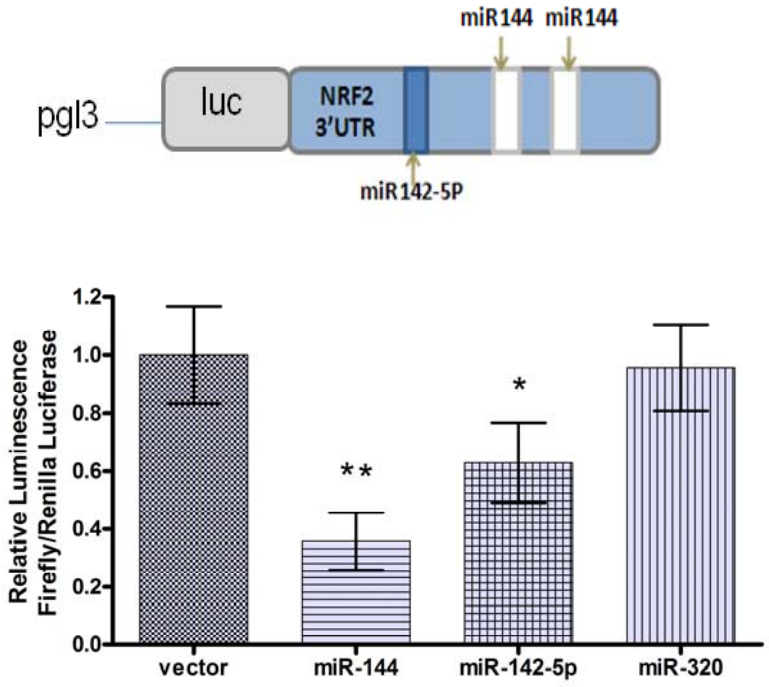
miR144
miR144
pgl3
luc
NRF2
3'UTR
miR142-5P
Relative Luminescence
Firefly/Renilla Luciferase
1.2
1.0
0.8
0.6
0.4
0.2
0.0
**
*
vector
miR-144
miR-142-5p
miR-320

Figure S5

A.

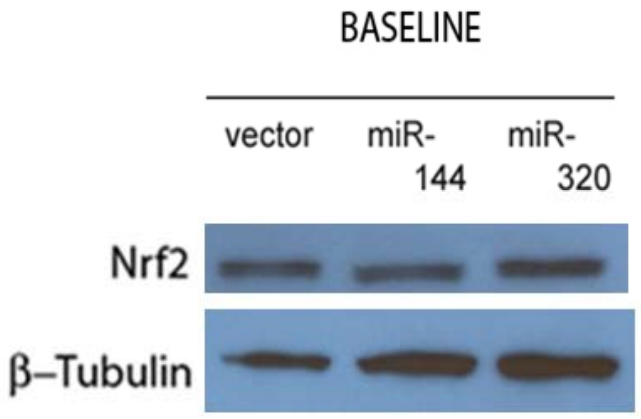

NRF2:β–Tubulin	.654	.359	.468

B.

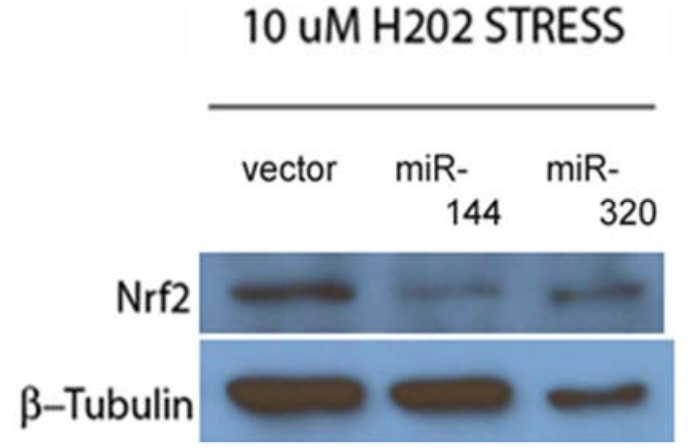

NRF2:β–Tubulin	.397	.138	.433

Figure S6

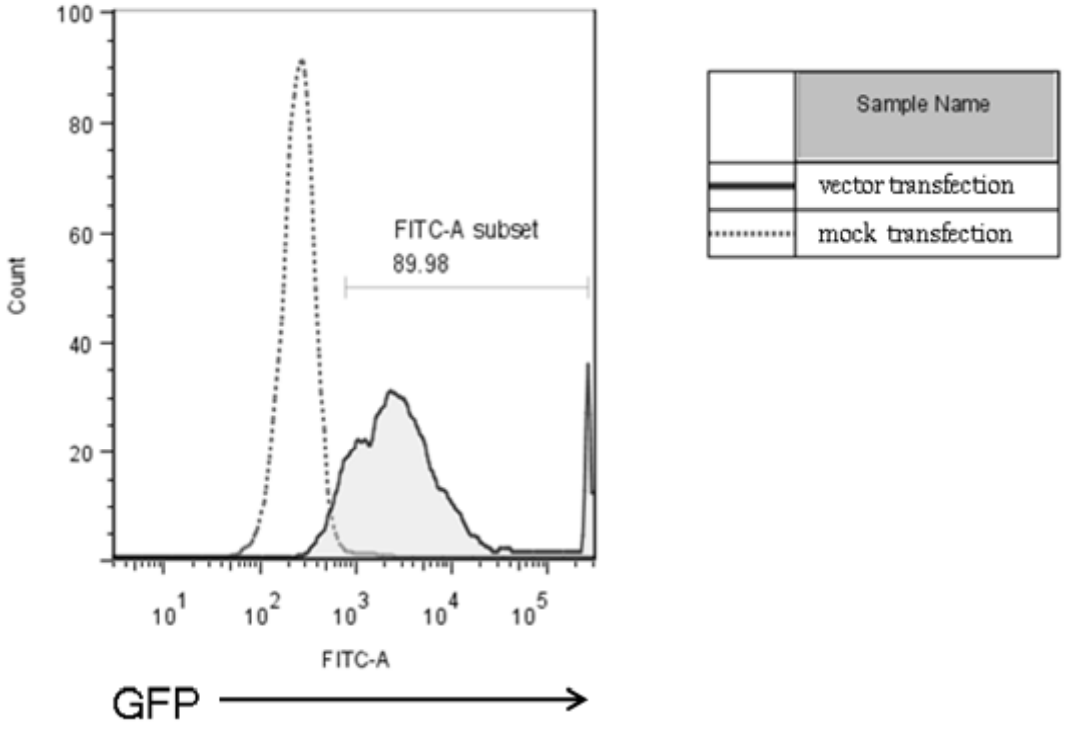
100
80
60
40
20
Count
FITC-A subset
89.98
10^1
10^2
10^3
10^4
10^5
FITC-A
GFP
Sample Name
vector transfection
mock transfection

Figure S7

A.

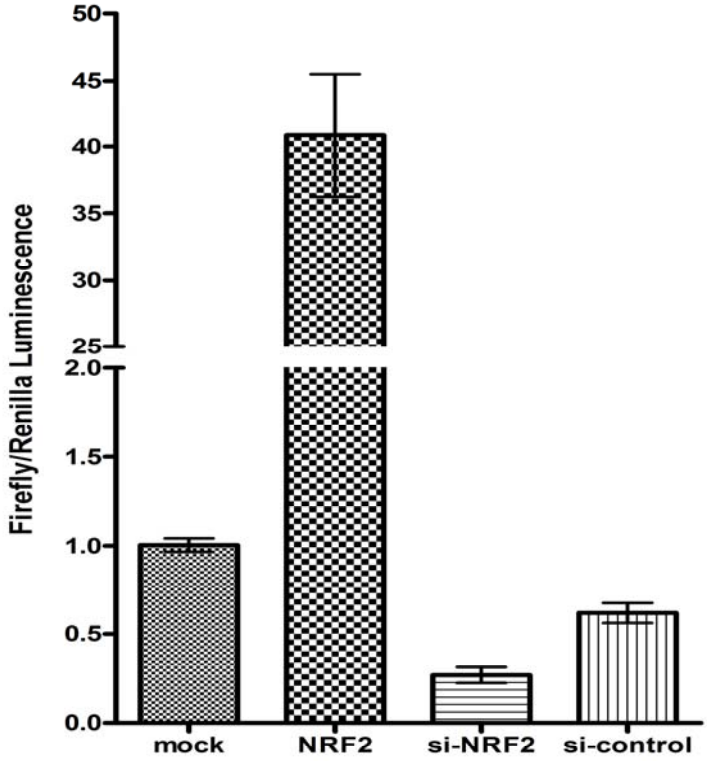

NQO1-ARE-luc	+	+	+	+
NRF2	--	+	--	--
si-control	--	--	--	+
si-NRF2	--	--	+	--

B.

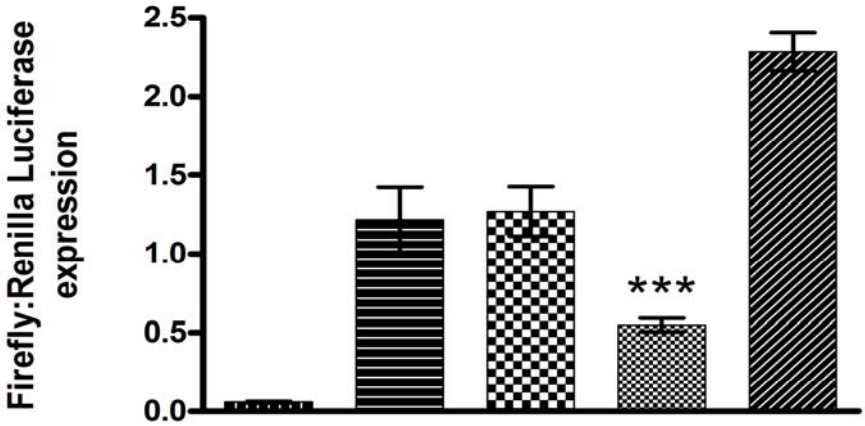

NQO1-ARE-luc	--	+	+	+	+
vector	--	--	+	+	--
miR-144	--	--	--	+	--
NRF2	--	--	--	--	+

Figure S8

A.

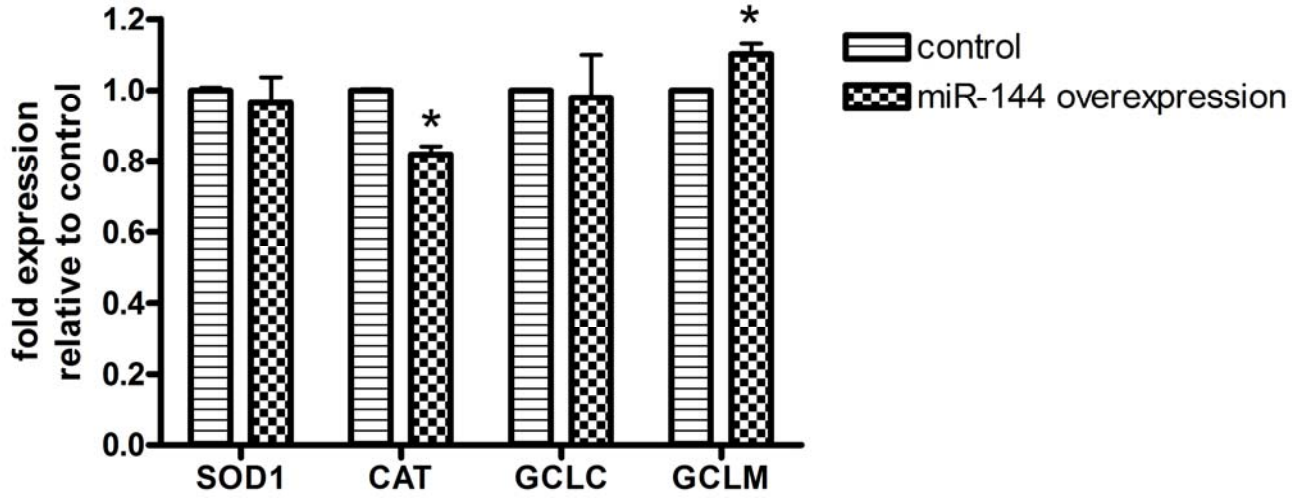
fold expression relative to control
1.2
1.0
0.8
0.6
0.4
0.2
0.0
*
*
SOD1
CAT
GCLC
GCLM
control
miR-144 overexpression

B.

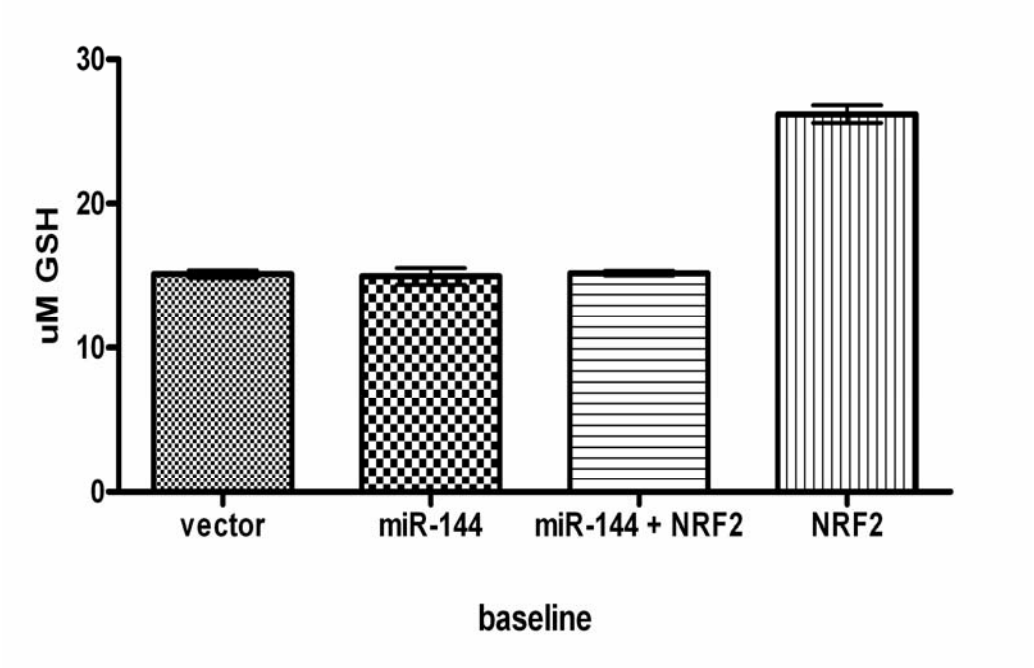
uM GSH
30
20
10
0
vector
miR-144
miR-144 + NRF2
NRF2
baseline

Figure S9

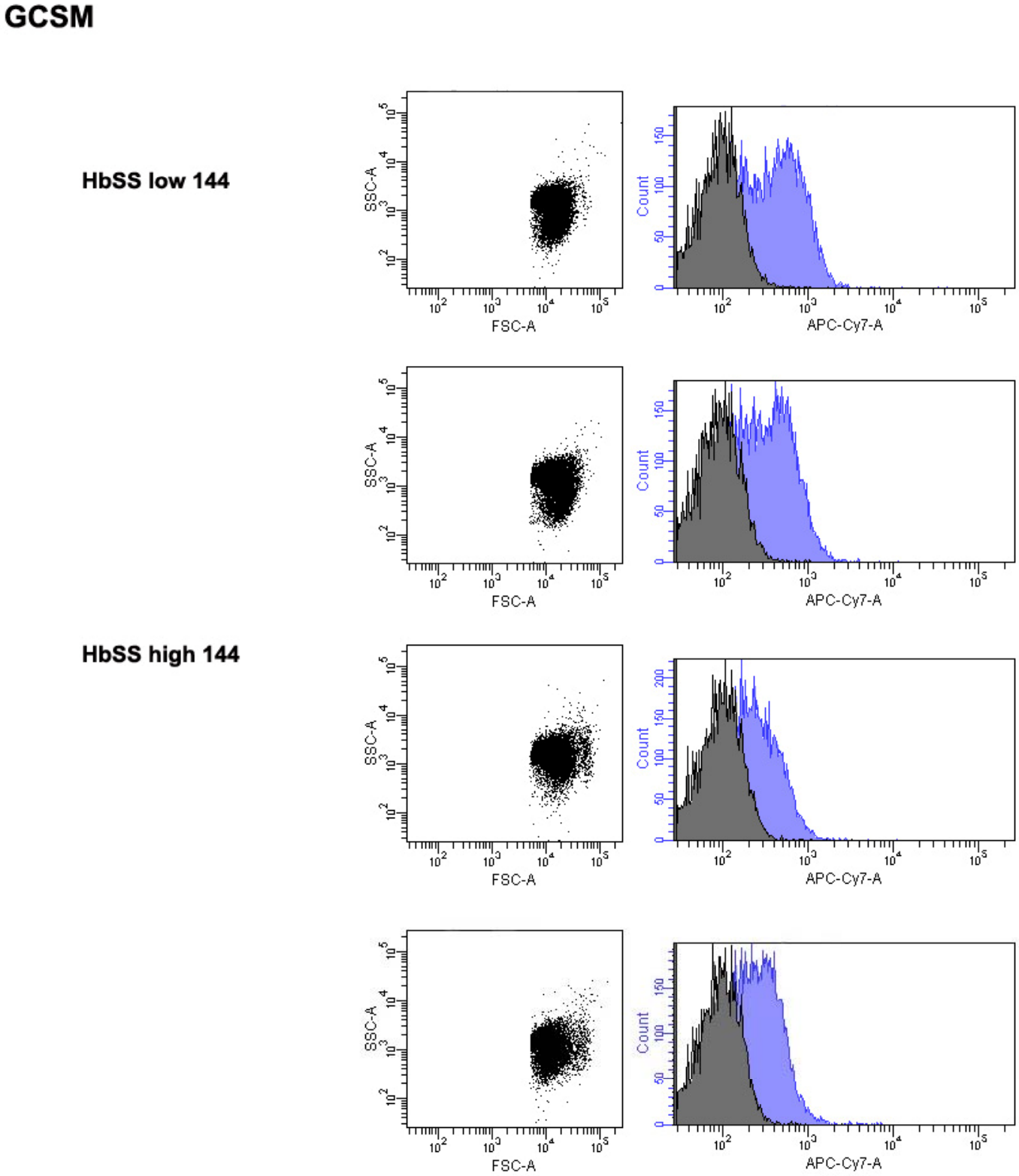

Figure S10

A.

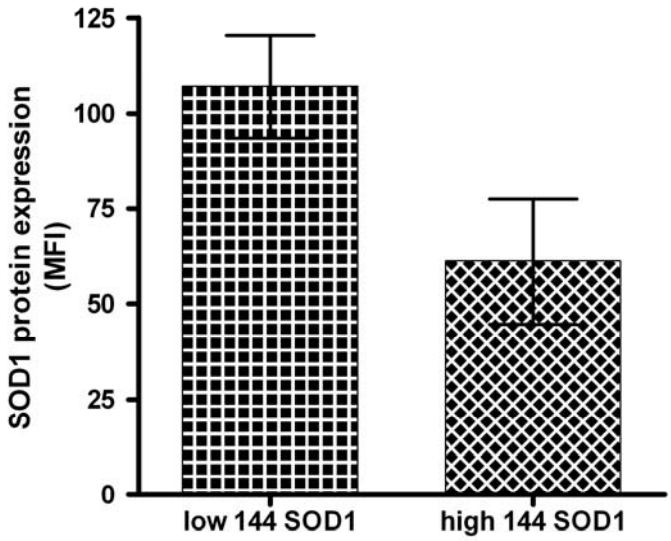

B.

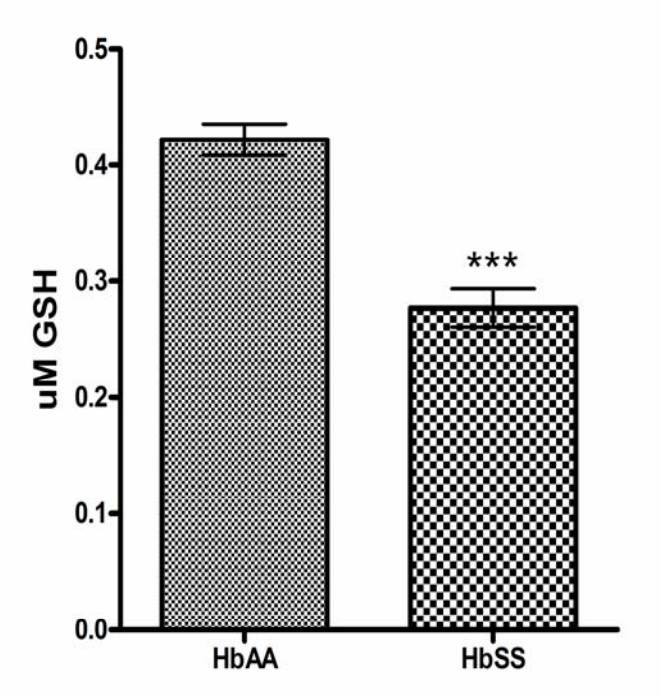

C.

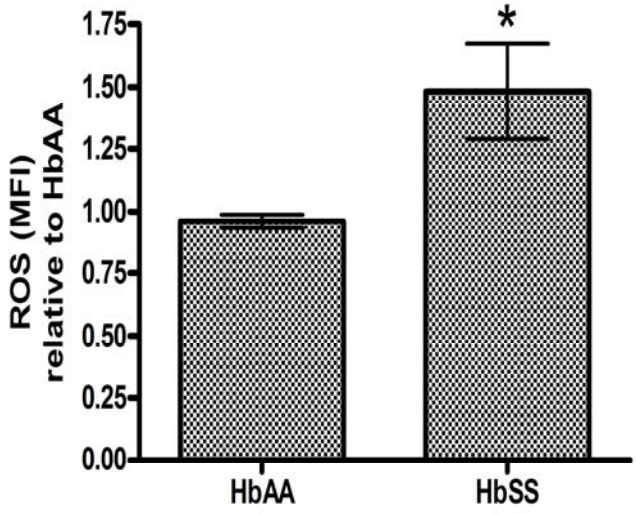

Figure S11

A.

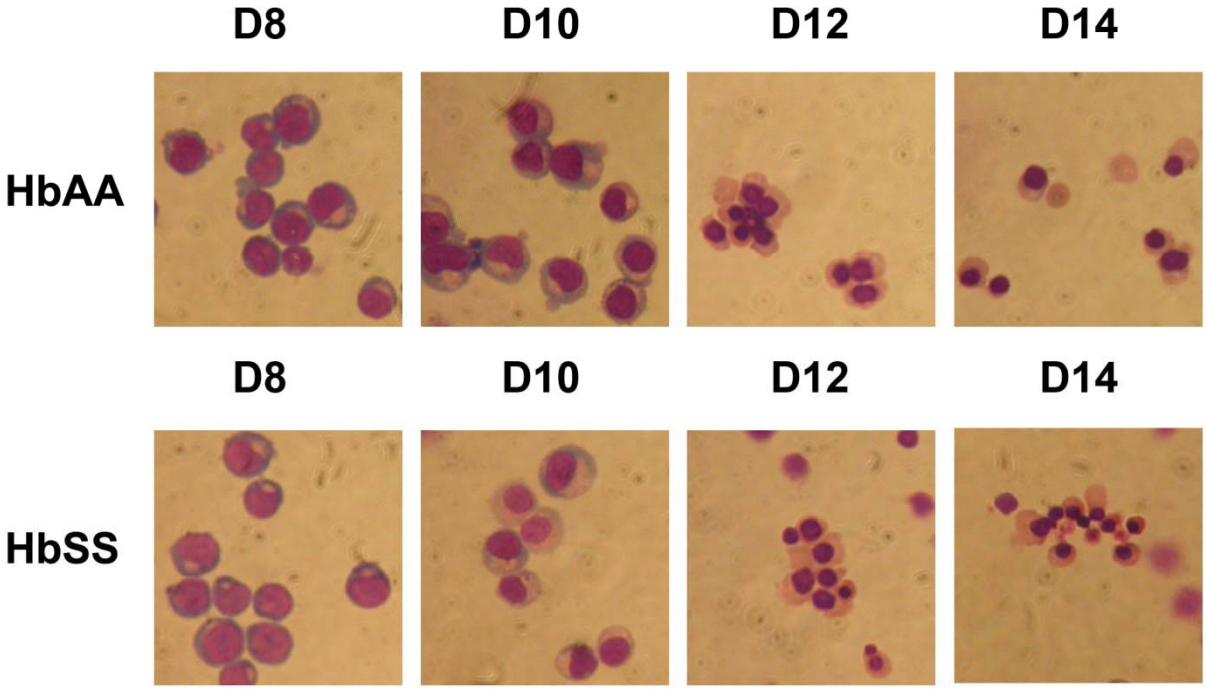

B.

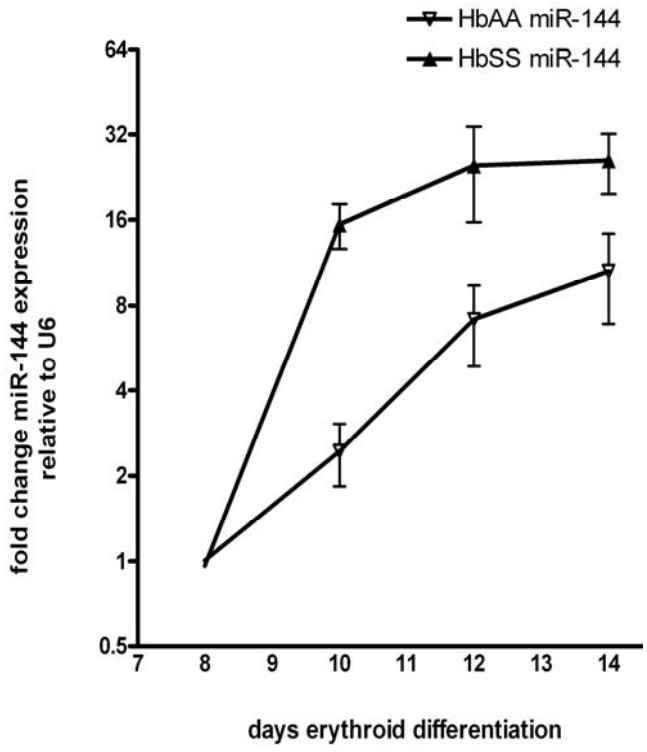

C.